

Is there new particle running in the loop-induced $H\gamma\gamma$ and Hgg vertex?

Seungwon Baek^{*}

School of Physics, KIAS, 85 Hoegiro, Seoul 02455, Korea

Xing-Bo Yuan[†]

Quantum Universe Center, KIAS, 85 Hoegiro, Seoul 02455, Korea

Physics Division, National Center for Theoretical Sciences, Hsinchu 300, Taiwan

Loop-induced Hgg and $H\gamma\gamma$ coupling play an important role in the Higgs production and decay at the LHC. These vertices can be affected by various New Physics contributions, including new particles, anomalous Yukawa couplings, and so on. We point out some ratios of the Higgs signal strengths could help disentangle the contributions of new particles from other sources of New Physics.

^{*}Electronic address: swbaek@kias.re.kr

[†]Electronic address: xbyuan@yonsei.ac.kr

I. INTRODUCTION

The first run of the LHC was very successful with the discovery of the Higgs boson [1, 2]. The measured couplings of the observed Higgs boson to fermions and gauge bosons are compatible with the Standard Model (SM) predictions at a typical $\mathcal{O}(10 - 20)\%$ precision level [3]. The next step would be precision Higgs coupling measurements, which will be performed at the Run II of the LHC and its high-luminosity upgrade [4, 5], as well as planned high-energy colliders [6, 7]. These precision measurements will allow more complete understanding of Electro-Weak Symmetry Breaking (EWSB) and are crucial for searching for physics Beyond the Standard Model (BSM) [8, 9].

BSM physics can contribute to all the Higgs couplings, including the couplings to fermions Hff and massive gauge bosons HVV , which control various Higgs production and decay channels at the LHC. Unlike the tree-level couplings, the Higgs couplings to photon $H\gamma\gamma$ and gluon Hgg are generated by loop diagrams in the SM. Therefore, they can be affected by BSM physics in a variety of ways [10, 11]. Generally, we can divide the various BSM sources into two scenarios. In the first scenario, the Hgg and $H\gamma\gamma$ couplings are affected only through the loop diagrams in the SM, where the Hff or HWW couplings are modified. In the second scenario, new particles also enter in the loop diagrams and affect the Hgg and $H\gamma\gamma$ couplings directly. Even if deviation of the rate for the gluon-gluon fusion production or $h \rightarrow \gamma\gamma$ decay were observed in the future, it is not straightforward to determine whether the anomaly is due to contributions from modified tree-level couplings or from new particles. One approach to probe these two different BSM sources would be to check if the SM tree-level coupling scale factors are sufficient to fit the Higgs data [12]. Alternatively, in this paper, we will build ratios from the Higgs signal strengths to disentangle the contributions of new particles from other BSM sources. All possible BSM contributions are parameterized in the framework of Effective Field Theory (EFT). Numerical analysis with the LHC Run I data is also performed.

This paper is organized as follows: In Sec. II, BSM contributions to the Higgs production and decay channels at the LHC are investigated in the EFT framework. Ratios of the Higgs signal strengths are built to analyze the BSM contributions. We present our numerical results in Sec. III and conclude in Sec. IV.

II. THEORETICAL FRAMEWORK

Considering current Higgs measurements at the LHC, a general theoretical framework can be provided by the effective Lagrangian [13, 14],

$$\begin{aligned} \mathcal{L} = & 2c_V \left(m_W^2 W_\mu^+ W^{-\mu} + \frac{1}{2} m_Z^2 Z_\mu Z^\mu \right) \frac{h}{v} + c_\gamma \frac{\alpha_e}{\pi} F_{\mu\nu} F^{\mu\nu} \frac{h}{v} + c_g \frac{\alpha_s}{12\pi} G_{\mu\nu}^a G^{a\mu\nu} \frac{h}{v} \\ & - c_t \frac{m_t}{v} \bar{t} t h - c_b \frac{m_b}{v} \bar{b} b h - c_c \frac{m_c}{v} \bar{c} c h - c_\tau \frac{m_\tau}{v} \bar{\tau} \tau h, \end{aligned} \quad (1)$$

with $v = 246 \text{ GeV}$. In the SM, the coupling c_f ($f = c, b, t, \tau$) and c_V ($V = W, Z$) are generated by tree-level diagrams and equal to unity, while c_γ and c_g arise at loop level and vanish here by definition. Note that c_γ and c_g are reserved only for new particle contributions. The contributions from the Hff or HVV are added separately. Generally, all these couplings could deviate from their SM values due to BSM physics. It is convenient to define the following effective couplings

$$\begin{aligned} C_f &= c_f, \\ C_V &= c_V, \\ C_\gamma &= c_\gamma - \frac{1}{8} \left(\sum_f c_f N_{c,f} Q_f^2 \mathcal{A}_{\frac{1}{2}}(x_f) + c_V \mathcal{A}_1(x_W) \right), \\ C_g &= c_g - \frac{3}{4} \sum_q c_q \mathcal{A}_{\frac{1}{2}}(x_q), \end{aligned} \quad (2)$$

where $x_f = 4m_f^2/m_h^2$, and the normalized ones

$$\kappa_i = C_i / C_i^{\text{SM}}. \quad (3)$$

The C_i^{SM} 's can be obtained from (2) by setting $c_f = c_V = 1, c_\gamma = c_g = 0$, and it turns out that $C_f^{\text{SM}} = C_V^{\text{SM}} = 1$, $C_\gamma^{\text{SM}} = -0.81$, and $C_g^{\text{SM}} = 0.99 + 0.07i$. Here the one-loop functions read [10, 15]

$$\begin{aligned} \mathcal{A}_{\frac{1}{2}}(x) &= -2x [1 + (1-x)f(x)], \\ \mathcal{A}_1(x) &= 2 + 3x + 3x(2-x)f(x), \end{aligned} \quad (4)$$

where

$$f(x) = \begin{cases} [\sin^{-1}(1/\sqrt{x})]^2, & x \geq 1, \\ -\frac{1}{4} \left[\log \left(\frac{1+\sqrt{1-x}}{1-\sqrt{1-x}} \right) - i\pi \right]^2, & x < 1. \end{cases} \quad (5)$$

These effective couplings describe the interactions of the Higgs boson to the SM fermions and gauge bosons, and can be straightforwardly used to investigate the Higgs observables, such as $\Gamma(h \rightarrow \gamma\gamma) \propto |C_\gamma|^2$ and $\sigma_{ggF} \propto |C_g|^2$. Generally, numerical results of these effective couplings are

$$\begin{aligned} C_\gamma &= c_\gamma + 0.23c_t - 1.04c_V, \\ C_g &= c_g + 1.04c_t - (0.05 - 0.07i)c_b, \end{aligned} \quad (6)$$

where the contributions from the light fermions c and τ are less than 1% and have been neglected. Fitting of C_i to various experimental data has been performed by several groups [16–20] to test the SM and also to search for the BSM.

In the BSM, the effective couplings C_i in eq. (2) may deviate from the SM values. Generally there are two scenarios:

Scenario I: $c_f, c_V \neq 1$ and $c_\gamma, c_g = 0$

Among the couplings c_i in eq. (1), only the Higgs couplings to the fermions and massive gauge bosons c_f and c_V are directly modified by the BSM contributions. Therefore, the BSM effects on the effective couplings to gluon and photon are implemented through the loop diagrams in the SM with the modified c_f and c_V , whose numerical results read

$$\begin{aligned} C_\gamma &= 0.23c_t - 1.04c_V, \\ C_g &= 1.04c_t - (0.05 - 0.07i)c_b. \end{aligned} \quad (7)$$

This scenario usually corresponds to the BSM models with large extra dimension [21] or BSM candidates without new electromagnetically charged particles coupled to Higgs such as gauged $L_\mu - L_\tau$ extensions of the SM [22, 23].

Scenario II: $c_f, c_V \neq 1$ and $c_\gamma, c_g \neq 0$

In some BSM candidates, new electrically charged or colored particles couple to the Higgs boson and generate loop-induced $H\gamma\gamma$ or Hgg couplings, which give rise to nonzero c_γ or c_g . In this scenario, the effective Higgs couplings to gluon and photon can be generally written as

$$\begin{aligned} C_\gamma &= c_\gamma + 0.23c_t - 1.04c_V, \\ C_g &= c_g + 1.04c_t - (0.05 - 0.07i)c_b. \end{aligned} \quad (8)$$

This scenario is the most general case, since all the couplings c_i could deviate from their SM values [24–26]. It is noted that nonzero c_γ can also be generated by the anomalous triple gauge coupling $W^+W^-\gamma$, which, however, is strongly constrained at high-energy colliders [27–33] or from the B and K meson decays [34, 35].

In the following, we will build some observables to discriminate these two scenarios.

At the LHC, Higgs boson production mainly occurs through the following channels,

gluon-gluon fusion (ggF) : $gg \rightarrow h$	coupling : C_g
vector boson fusion (VBF) : $qq \rightarrow qqh$	coupling : C_V
associated production (VH) : $qq \rightarrow W/Zh$	coupling : C_V
associated production (ttH) : $qq/gg \rightarrow tth$	coupling : C_t ,

where the effective couplings relevant for each process are also listed. It is noted that, associated production with a Z boson also includes a process $gg \rightarrow Zh$ induced by top quark loops, which are affected by the effective coupling C_t [3]. For simplicity, we only consider the associated production with a W boson in the following. In this work, the most relevant decay modes of the Higgs boson are listed below:

decay : $h \rightarrow \gamma\gamma$	coupling : C_γ
decay : $h \rightarrow WW^*/ZZ^*$	coupling : C_V
decay : $h \rightarrow bb/\tau\tau$	coupling : C_b, C_τ

The SM predictions on the Higgs production cross sections and decay branching ratios have been summarized in refs. [12, 36, 37].

To characterise the Higgs boson property, a signal strength is usually defined for a particular Higgs production and decay process $i \rightarrow h \rightarrow j$ at the LHC [3],

$$\mu_i = \frac{\sigma_i}{\sigma_i^{\text{SM}}}, \quad \mu^j = \frac{\mathcal{B}_j}{\mathcal{B}_j^{\text{SM}}}, \quad \mu_i^j = \mu_i \cdot \mu^j \quad (9)$$

where σ_i ($i = ggF, VBF, WH, ZH, ttH$) and \mathcal{B}_j ($j = ZZ^*, WW^*, \gamma\gamma, \tau\tau, bb$) are the production cross section for $i \rightarrow h$ and the branching ratio of the decay $h \rightarrow j$, respectively. Observables with the superscript “SM” indicate their SM predictions. Therefore, $\mu_i = 1$, $\mu^j = 1$ and $\mu_i^j = 1$ in the SM. It is straightforward to represent the signal strengths with the normalized couplings defined in eq. (3), which read

$$\mu_{ggF} = |\kappa_g|^2, \quad \mu_{VBF} = |\kappa_V|^2, \quad \mu_{WH} = |\kappa_V|^2, \quad \mu_{ttH} = |\kappa_t|^2, \quad (10)$$

and

$$\mu^{VV} = \frac{|\kappa_V|^2}{r_\Gamma}, \quad \mu^{\gamma\gamma} = \frac{|\kappa_\gamma|^2}{r_\Gamma}, \quad \mu^{ff} = \frac{|\kappa_f|^2}{r_\Gamma}, \quad (11)$$

with $r_\Gamma = \Gamma_H/\Gamma_H^{\text{SM}}$. Here, Γ_H denotes the total decay width of the Higgs boson and depends on all the couplings in the effective Lagrangian eq. (1).

Instead of the signal strengths themselves, it is interesting to consider their ratios, which can get rid of the total Higgs decay width [38–46]. Among all possible combinations, ratios of the signal strengths with same production or decay mode are the simplest, such as the ratios defined below

$$r_{1,V}^j = \frac{\mu_{ggF}^j}{\mu_V^j}, \quad r_{2,i} = \frac{\mu_i^{\gamma\gamma}}{\mu_i^{VV}}, \quad r_3^j = \frac{\mu_{ggF}^j}{\mu_{ttH}^j}, \quad (12)$$

where V denotes the VBF or WH production mode. Since either the decay or production signal strength is canceled in each ratio, we can reduce them to the following basic ones

$$r_1 = \frac{\mu_{ggF}}{\mu_V}, \quad r_2 = \frac{\mu^{\gamma\gamma}}{\mu^{VV}}, \quad r_3 = \frac{\mu_{ggF}}{\mu_{ttH}}. \quad (13)$$

With eq. (10) and (11), it's easy to obtain

$$r_1 = r_{1,V}^j = \left| \frac{\kappa_g}{\kappa_V} \right|^2, \quad r_2 = r_{2,i} = \left| \frac{\kappa_\gamma}{\kappa_V} \right|^2, \quad r_3 = r_3^j = \left| \frac{\kappa_g}{\kappa_t} \right|^2. \quad (14)$$

In *scenarios I* and *II*, their numerical results read

	Scenario I	Scenario II
$r_1 =$	$\left 1.06 \frac{c_t}{c_V} \right ^2,$	$\left 1.06 \frac{c_t}{c_V} + 1.03 \frac{c_g}{c_V} \right ^2,$
$r_2 =$	$\left -1.27 + 0.28 \frac{c_t}{c_V} \right ^2,$	$\left -1.27 + 0.28 \frac{c_t}{c_V} + 1.2 \frac{c_\gamma}{c_V} \right ^2,$
$r_3 =$	$ 1.06 ^2,$	$\left 1.06 + 1.03 \frac{c_g}{c_t} \right ^2,$

(15)

where the contribution from b quark has been neglected. In *scenario I*, the ratios r_1 and r_2 only depend on one parameter c_t/c_V , and the ratio r_3 is a constant. So these three ratios are strongly correlated with each other. In *scenario II*, however, the ratios receive additional contributions from c_γ or c_g , and the correlation between them no longer exists. Therefore, it is possible to distinguish between *scenario I* and *II* by investigating the correlations between the ratios r_1 , r_2 and r_3 .

Before presenting the numerical analysis, a few comments are given here:

- When obtaining the numerical results of r_1 , r_2 and r_3 in eq. (15), the contribution from b quark is neglected. Since it only accounts for around 10% of the effective coupling of the Higgs boson to gluon C_g , the one-parameter correlation between r_1 , r_2 and r_3 in *scenario I* is not polluted so much even after including this contribution. Furthermore, in the case that the Yukawa couplings c_f are universal, the correlations in *scenario I* hold exactly.
- As advocated in refs. [38, 39], theoretical uncertainties in the ratios r_i are largely eliminated, since either same production or decay channels are taken. Furthermore, some systematic errors, such as the one related with luminosity measurements, also cancel out in the ratios.
- In the effective Lagrangian eq. (1), the BSM contributions to the tree-level Hff and HVV vertices are equivalent to multiplicative overall factors. Therefore, their QCD corrections cancel in the relevant signal strengths. For loop-induced vertices, the QCD corrections have been computed up to N³LO for $gg \rightarrow h$ [47–56] and NLO for $h \rightarrow \gamma\gamma$ [56–63], and the NLO EW corrections are also available [64–69]. Although they modify the effective couplings C_g and C_γ by around 10% level, their effects appear in both the denominator and numerator and are expected to be largely canceled in the signal strengths μ_{ggF} and $\mu^{\gamma\gamma}$. We leave the high-order QCD and EW corrections to the ratios r_{1-3} for future work.
- It is possible to define other ratios which present similar features as r_{1-3} , such as $\mu_{ggF}^{VV}/\mu_V^{\gamma\gamma}$. For simplicity, these ratios are not included in this paper.

III. NUMERICAL ANALYSIS

As discussed in the previous section, the correlations between the ratios r_i in *scenario I* are slightly polluted by the contributions from light fermions. To account for such contributions, we perform numerical analysis in two cases: the scale factors for the Yukawa couplings are universal or non-universal, which correspond to the following parameter sets:

	universal coupling	non-universal coupling
<i>scenario I</i>	(c_V, c_F)	(c_V, c_b, c_t, c_τ)
<i>scenario II</i>	$(c_V, c_F, c_\gamma, c_g)$	$(c_V, c_b, c_t, c_\tau, c_\gamma, c_g)$.

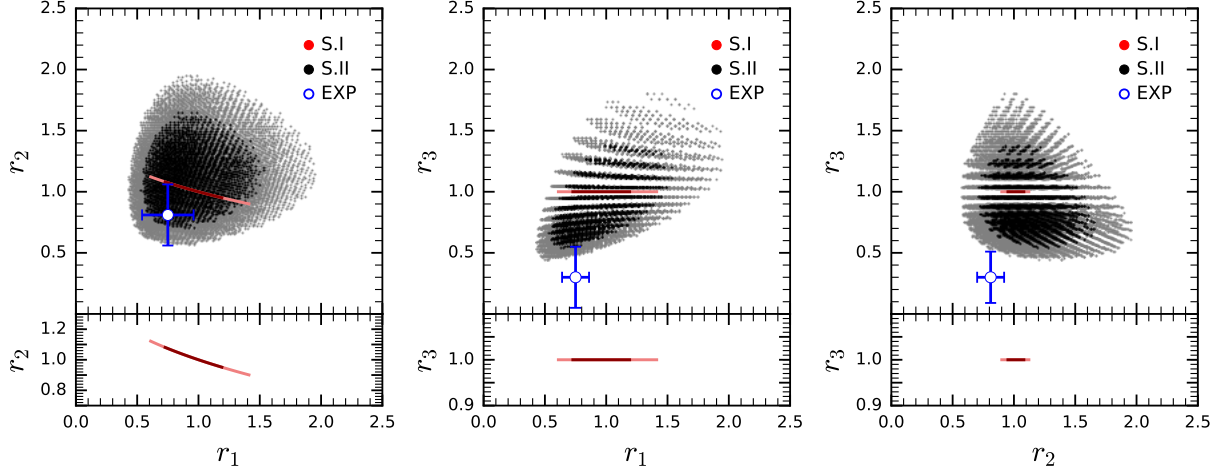


FIG. 1: Correlations between the ratios r_1 , r_2 and r_3 in the case of universal scale factors for the Yukawa couplings, which are obtained from the allowed parameter space S.I (c_V, c_F) (dark red: 68% CL, light red: 95% CL) and S.II (c_V, c_F, c_γ, c_g) (black: 68% CL, gray: 95% CL). The experimental data with 1σ error is illustrated by the blue point. Scaled plot for r_2 and r_3 are also shown below each figure.

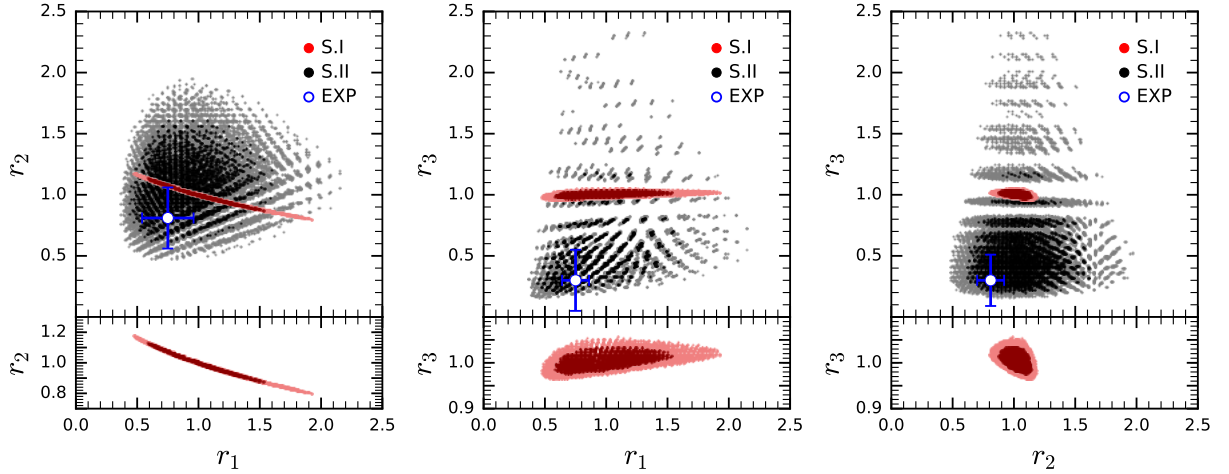


FIG. 2: As in Fig. 1, but from the parameter space S.I (c_V, c_b, c_t, c_τ) and S.II ($c_V, c_b, c_t, c_\tau, c_\gamma, c_g$).

We perform a global fit for each parameter set. The package `Lilith-1.1.3` with database DB 15.09 [70] is used to take into account the Higgs signal strengths measured by LHC Run I [71, 72] and Tevatron [73]. Our parameter scan doesn't include the LHC Run II data, since the corresponding Higgs signal strengths haven't been fully available yet [74, 75]. Our global fit shows that $\mathcal{O}(20\%)$ deviations from the SM values are allowed in the fit of (c_V, c_F) , while $\mathcal{O}(50\%)$ in the other three fits. The fit results for the parameter set (c_V, c_F) and $(c_V, c_b, c_t, c_\tau, c_\gamma, c_g)$ can also be found in ref. [3] and [76], respectively.

We can obtain the experimental values of r_1 , r_2 and r_3 from the following ratios.

	$\sigma_{VBF}/\sigma_{ggF}$	$\mathcal{B}^{\gamma\gamma}/\mathcal{B}^{ZZ}$	$\sigma_{ttH}/\sigma_{ggF}$
SM [12]	0.082 ± 0.009	0.0854 ± 0.0010	0.0067 ± 0.0010
EXP [3]	0.109 ± 0.034	0.069 ± 0.018	0.022 ± 0.007

To be conservative, experimental errors have been symmetrized. Compared to the SM predictions, the current experimental uncertainties are rather large, which are mainly due to the limited statistics available [3] and expected to be improved significantly at the future LHC.

In the case of universal scale factors for the Yukawa couplings, the ratios r_i in *scenario I* and *II* are shown in Fig. 1. In *scenario I*, as expected, r_1 and r_2 is strongly correlated with each other and r_3 is kept a constant. However, the three ratios can vary independently in a wide range in *scenario II*. The numerical results in the case of the non-universal scale factors are shown in Fig. 2. Although the contributions from light fermions are included generally, the correlation between r_1 and r_2 in *scenario I* is still very strong and r_3 can depart from its SM value by at most 5%. Considering the LHC Run I data, the measured ratios prefer *scenario II*, but with large uncertainty. At the future LHC, any observed deviation from the correlations in *scenario I* would indicate non-vanishing coupling c_γ or c_g , which can provide a hint of new particles running in the loop of the $H\gamma\gamma$ or Hgg coupling.

IV. CONCLUSIONS

In this paper, we have investigated how to use the Higgs observables at the LHC to determine if new particles enter the loops of the $H\gamma\gamma$ and Hgg effective couplings. Accordingly, we considered two general BSM scenarios. In *scenario I*, only tree-level Higgs couplings to fermions and massive gauge bosons are affected. They can still change the $H\gamma\gamma$ and Hgg couplings through the corresponding SM loop diagrams. In *scenario II*, besides the modified tree-level couplings, there are new particles which can enter in the loop-induced vertices and they modify the $H\gamma\gamma$ and Hgg couplings directly.

Effects of these two BSM scenarios on the Higgs observables at the LHC have been investigated in the EFT framework. We have constructed ratios of the Higgs signal strengths to distinguish between the two scenarios. We find that, in *scenario I*, the ratios $r_1 = \mu_{ggF}/\mu_V$ and $r_2 = \mu^{\gamma\gamma}/\mu^{VV}$ strongly correlate with each other and $r_3 = \mu_{ggF}/\mu_{ttH}$ can deviate from

its SM value by at most 5%. However, the ratios in *scenario II* vary independently in a wide range. Due to these different features, the ratios can provide information on whether there are new particles running in the loops of Hgg and $H\gamma\gamma$ vertices. With large statistics expected at the future LHC, these ratios can be determined with a high precision, which makes them powerful tools to analysis possible anomalous Higgs couplings.

Acknowledgments

SB is supported in part by National Research Foundation of Korea (NRF) Research Grant NRF-2015R1A2A1A05001869. XY is supported by NCTS. XY thanks Xiao-Gang He, Yun Jiang and Pyungwon Ko for useful discussions, and KIAS and QUC for its hospitality, where this work was mainly conducted. We thank J  r  my Bernon for explaining the `Lilith` code.

-
- [1] G. Aad et al. (ATLAS), Phys. Lett. **B716**, 1 (2012), 1207.7214.
 - [2] S. Chatrchyan et al. (CMS), Phys. Lett. **B716**, 30 (2012), 1207.7235.
 - [3] G. Aad et al. (ATLAS, CMS), JHEP **08**, 045 (2016), 1606.02266.
 - [4] A. Collaboration (ATLAS), in *Proceedings, Community Summer Study 2013: Snowmass on the Mississippi (CSS2013): Minneapolis, MN, USA, July 29-August 6, 2013* (2013), 1307.7292, URL <http://inspirehep.net/record/1245017/files/arXiv:1307.7292.pdf>.
 - [5] C. Collaboration (CMS), in *Proceedings, Community Summer Study 2013: Snowmass on the Mississippi (CSS2013): Minneapolis, MN, USA, July 29-August 6, 2013* (2013), 1307.7135, URL <http://inspirehep.net/record/1244669/files/arXiv:1307.7135.pdf>.
 - [6] H. Baer, T. Barklow, K. Fujii, Y. Gao, A. Hoang, S. Kanemura, J. List, H. E. Logan, A. Nomerotski, M. Perelstein, et al. (2013), 1306.6352.
 - [7] C.-S. S. Group (2015).
 - [8] C. Csaki, C. Grojean, and J. Terning, Rev. Mod. Phys. **88**, 045001 (2016), 1512.00468.
 - [9] C. Mariotti and G. Passarino (2016), 1612.00269.
 - [10] J. F. Gunion, H. E. Haber, G. L. Kane, and S. Dawson, Front. Phys. **80**, 1 (2000).
 - [11] S. Dawson et al., in *Proceedings, 2013 Community Summer Study on the Future of U.S. Particle Physics: Snowmass on the Mississippi (CSS2013): Minneapolis, MN, USA, July*

- 29-August 6, 2013* (2013), 1310.8361.
- [12] J. R. Andersen et al. (LHC Higgs Cross Section Working Group) (2013), 1307.1347.
 - [13] D. Carmi, A. Falkowski, E. Kuflik, T. Volansky, and J. Zupan, JHEP **10**, 196 (2012), 1207.1718.
 - [14] G. Buchalla, O. Cata, A. Celis, and C. Krause, Phys. Lett. **B750**, 298 (2015), 1504.01707.
 - [15] A. Djouadi, Phys. Rept. **457**, 1 (2008), hep-ph/0503172.
 - [16] G. Belanger, B. Dumont, U. Ellwanger, J. F. Gunion, and S. Kraml, JHEP **02**, 053 (2013), 1212.5244.
 - [17] G. Belanger, B. Dumont, U. Ellwanger, J. F. Gunion, and S. Kraml, Phys. Rev. **D88**, 075008 (2013), 1306.2941.
 - [18] J. Ellis and T. You, JHEP **06**, 103 (2013), 1303.3879.
 - [19] P. P. Giardino, K. Kannike, I. Masina, M. Raidal, and A. Strumia, JHEP **05**, 046 (2014), 1303.3570.
 - [20] S. Fichet and G. Moreau, Nucl. Phys. **B905**, 391 (2016), 1509.00472.
 - [21] N. Maru and N. Okada (2016), 1604.01150.
 - [22] S. Baek, N. G. Deshpande, X. G. He, and P. Ko, Phys. Rev. **D64**, 055006 (2001), hep-ph/0104141.
 - [23] S. Baek, Phys. Lett. **B756**, 1 (2016), 1510.02168.
 - [24] L. G. Almeida, E. Bertuzzo, P. A. N. Machado, and R. Zukanovich Funchal, JHEP **11**, 085 (2012), 1207.5254.
 - [25] S. Baek and K. Nishiwaki, Phys. Rev. **D93**, 015002 (2016), 1509.07410.
 - [26] S. Baek and Z.-F. Kang, JHEP **03**, 106 (2016), 1510.00100.
 - [27] S. Schael et al. (DELPHI, OPAL, LEP Electroweak, ALEPH, L3), Phys. Rept. **532**, 119 (2013), 1302.3415.
 - [28] T. A. Aaltonen et al. (CDF), Phys. Rev. **D91**, 111101 (2015), [Addendum: Phys. Rev.D92,no.3,039901(2015)], 1505.00801.
 - [29] T. A. Aaltonen et al. (CDF), Phys. Rev. **D94**, 032008 (2016), 1606.06823.
 - [30] G. Aad et al. (ATLAS), JHEP **09**, 029 (2016), 1603.01702.
 - [31] V. Khachatryan et al. (CMS), Eur. Phys. J. **C76**, 401 (2016), 1507.03268.
 - [32] A. Falkowski, M. Gonzalez-Alonso, A. Greljo, and D. Marzocca, Phys. Rev. Lett. **116**, 011801 (2016), 1508.00581.

- [33] A. Falkowski, M. Gonzalez-Alonso, A. Greljo, D. Marzocca, and M. Son (2016), 1609.06312.
- [34] X.-G. He and B. McKellar, Phys. Lett. **B320**, 165 (1994), hep-ph/9309228.
- [35] C. Bobeth and U. Haisch, JHEP **09**, 018 (2015), 1503.04829.
- [36] S. Dittmaier et al. (LHC Higgs Cross Section Working Group) (2011), 1101.0593.
- [37] S. Dittmaier et al. (2012), 1201.3084.
- [38] D. Zeppenfeld, R. Kinnunen, A. Nikitenko, and E. Richter-Was, Phys. Rev. **D62**, 013009 (2000), hep-ph/0002036.
- [39] A. Djouadi, Eur. Phys. J. **C73**, 2498 (2013), 1208.3436.
- [40] A. Djouadi, J. Quevillon, and R. Vega-Morales, Phys. Lett. **B757**, 412 (2016), 1509.03913.
- [41] J. F. Gunion, Y. Jiang, and S. Kraml, Phys. Rev. **D86**, 071702 (2012), 1207.1545.
- [42] J. F. Gunion, Y. Jiang, and S. Kraml, Phys. Rev. Lett. **110**, 051801 (2013), 1208.1817.
- [43] P. M. Ferreira, R. Santos, H. E. Haber, and J. P. Silva, Phys. Rev. **D87**, 055009 (2013), 1211.3131.
- [44] Y. Grossman, Z. Surujon, and J. Zupan, JHEP **03**, 176 (2013), 1301.0328.
- [45] S. Chang, S. K. Kang, J.-P. Lee, K. Y. Lee, S. C. Park, and J. Song, JHEP **05**, 075 (2013), 1210.3439.
- [46] F. Goertz, A. Papaefstathiou, L. L. Yang, and J. Zurita, JHEP **06**, 016 (2013), 1301.3492.
- [47] K. G. Chetyrkin, B. A. Kniehl, and M. Steinhauser, Nucl. Phys. **B510**, 61 (1998), hep-ph/9708255.
- [48] M. Kramer, E. Laenen, and M. Spira, Nucl. Phys. **B511**, 523 (1998), hep-ph/9611272.
- [49] Y. Schroder and M. Steinhauser, JHEP **01**, 051 (2006), hep-ph/0512058.
- [50] K. G. Chetyrkin, J. H. Kuhn, and C. Sturm, Nucl. Phys. **B744**, 121 (2006), hep-ph/0512060.
- [51] P. A. Baikov and K. G. Chetyrkin, Phys. Rev. Lett. **97**, 061803 (2006), hep-ph/0604194.
- [52] T. Inami, T. Kubota, and Y. Okada, Z. Phys. **C18**, 69 (1983).
- [53] A. Djouadi, M. Spira, and P. M. Zerwas, Phys. Lett. **B264**, 440 (1991).
- [54] K. G. Chetyrkin, B. A. Kniehl, and M. Steinhauser, Phys. Rev. Lett. **79**, 353 (1997), hep-ph/9705240.
- [55] C. Anastasiou, C. Duhr, F. Dulat, F. Herzog, and B. Mistlberger, Phys. Rev. Lett. **114**, 212001 (2015), 1503.06056.
- [56] M. Spira, A. Djouadi, D. Graudenz, and P. M. Zerwas, Nucl. Phys. **B453**, 17 (1995), hep-ph/9504378.

- [57] A. Djouadi, M. Spira, and P. M. Zerwas, Phys. Lett. **B311**, 255 (1993), hep-ph/9305335.
- [58] H.-Q. Zheng and D.-D. Wu, Phys. Rev. **D42**, 3760 (1990).
- [59] A. Djouadi, M. Spira, J. J. van der Bij, and P. M. Zerwas, Phys. Lett. **B257**, 187 (1991).
- [60] S. Dawson and R. P. Kauffman, Phys. Rev. **D47**, 1264 (1993).
- [61] K. Melnikov and O. I. Yakovlev, Phys. Lett. **B312**, 179 (1993), hep-ph/9302281.
- [62] M. Inoue, R. Najima, T. Oka, and J. Saito, Mod. Phys. Lett. **A9**, 1189 (1994).
- [63] J. Fleischer, O. V. Tarasov, and V. O. Tarasov, Phys. Lett. **B584**, 294 (2004), hep-ph/0401090.
- [64] U. Aglietti, R. Bonciani, G. Degrassi, and A. Vicini, Phys. Lett. **B595**, 432 (2004), hep-ph/0404071.
- [65] U. Aglietti, R. Bonciani, G. Degrassi, and A. Vicini, Phys. Lett. **B600**, 57 (2004), hep-ph/0407162.
- [66] S. Actis, G. Passarino, C. Sturm, and S. Uccirati, Nucl. Phys. **B811**, 182 (2009), 0809.3667.
- [67] G. Degrassi and F. Maltoni, Phys. Lett. **B600**, 255 (2004), hep-ph/0407249.
- [68] S. Actis, G. Passarino, C. Sturm, and S. Uccirati, Phys. Lett. **B670**, 12 (2008), 0809.1301.
- [69] G. Degrassi and F. Maltoni, Nucl. Phys. **B724**, 183 (2005), hep-ph/0504137.
- [70] J. Bernon and B. Dumont, Eur. Phys. J. **C75**, 440 (2015), 1502.04138.
- [71] T. ATLAS and C. Collaborations, ATLAS-CONF-2015-044 (2015).
- [72] C. Collaboration (CMS), CMS-PAS-HIG-15-002 (2015).
- [73] T. Aaltonen et al. (CDF, D0), Phys. Rev. **D88**, 052014 (2013), 1303.6346.
- [74] C. Gemme (2016), 1612.01987.
- [75] E. Palencia Cortezon (CMS), in *9th International Workshop on Top Quark Physics (TOP 2016) Olomouc, Czech Republic, September 19-23, 2016* (2016), 1612.00946, URL <http://inspirehep.net/record/1501679/files/arXiv:1612.00946.pdf>.
- [76] G. Buchalla, O. Cata, A. Celis, and C. Krause, Eur. Phys. J. **C76**, 233 (2016), 1511.00988.